Article

Remotely-Sensed Early Warning Signals of a Critical Transition in a Wetland Ecosystem

Sara Alibakhshi [1,*], Thomas A. Groen [2], Miina Rautiainen [1,3] and Babak Naimi [4,5]

[1] Department of Built Environment, School of Engineering, Aalto University, P.O. Box 14100, 00076 Espoo, Finland; miina.a.rautiainen@aalto.fi

[2] Faculty of Geo-Information Science and Earth Observation (ITC), University of Twente, P.O. Box 217, 7500 AE Enschede, The Netherlands; t.a.groen@utwente.nl

[3] Department of Electronics and Nanoengineering, School of Electrical Engineering, Aalto University, P.O. Box 14100, 00076 Espoo, Finland

[4] Center for Macroecology, Evolution and Climate (CMEC), Natural History Museum of Denmark, University of Copenhagen, Universitetparken 15, DK-2100 Copenhagen, Denmark; naimi.b@gmail.com

[5] Department of Environment and Energy, Science and Research Branch, Islamic Azad University, Tehran, Iran

[*] Correspondence: sara.alibakhshi@aalto.fi; Tel.: +358-469-386-186

Abstract: The response of an ecosystem to external drivers may not always be gradual and reversible. Discontinuous and sometimes irreversible changes, called 'regime shifts' or 'critical transitions', can occur. The likelihood of such shifts is expected to increase for a variety of ecosystems, and it is difficult to predict how close an ecosystem is to a critical transition. Recent modelling studies identified indicators of impending regime shifts that can be used to provide early warning signals of a critical transition. The identification of such transitions crucially depends on the ability to monitor key ecosystem variables, and their success may be limited by lack of appropriate data. Moreover, empirical demonstrations of the actual functioning of these indicators in real-world ecosystems are rare. This paper presents the first study which uses remote sensing data to identify a critical transition in a wetland ecosystem. In this study, we argue that a time series of remote sensing data can help to characterize and determine the timing of a critical transition. This can enhance our abilities to detect and anticipate them. We explored the potentials of remotely sensed vegetation (NDVI), water (MNDWI), and vegetation-water (VWR) indices, obtained from time series of MODIS satellite images to characterize the stability of a wetland ecosystem, Dorge Sangi, near the lake Urmia, Iran, that experienced a regime shift recently. In addition, as a control case, we applied the same methods to another wetland ecosystem in Lake Arpi, Armenia which did not experience a regime shift. We propose a new composite index (MVWR) based on combining vegetation and water indices, which can improve the ability to anticipate a critical transition in a wetland ecosystem. Our results revealed that MVWR in combination with autocorrelation at-lag-1 could successfully provide early warning signals for a critical transition in a wetland ecosystem, and showed a significantly improved performance compared to either vegetation (NDVI) or water (MNDWI) indices alone.

Keywords: critical transitions; early warning signals; resilience; time series; modified vegetation water index; spectral index; wetland; MNDWI

1. Introduction

Human activities may invoke gradual but profound changes to ecosystems such as coral reefs, lakes, wetlands and forests. The response of an ecosystem to such changes may not always be gradual, predictable, and reversible, but might instead be nonlinear, abrupt and irreversible [1]. Such changes

are also called abrupt shifts, regime shifts or critical transitions. Critical transitions occur when ecosystems are not resilient and cannot cope with external stresses [2]. When the resilience of an ecosystem decreases, the ecosystem will be slower in recovering from small disturbances until it is so close to a critical threshold, that is also called a 'tipping point'. Under such a situation, even a small perturbation can invoke a critical transition to another state where returning to the previous state can be difficult and sometimes impossible [3].

As a consequence of increasing natural and human-caused changes, the likelihood of critical transitions is expected to increase for many ecosystems [2,4–6]. However, it is hard to predict how close a system is to a tipping point and when a critical transition is going to occur [7]. Theories of critical transitions suggest that variables representing the state of an ecosystem change predictably before critical transitions. These state variables can therefore provide early warning signals of the upcoming transition [8]. This change, in advance of a critical transition, refers to a dynamic phenomenon—'critical slowing down'—defined as decreased recovery rates when the resilience of an ecosystem is low [9]. A number of methods have been developed that measure critical slowing down. These methods are statistical indicators that characterize time series of a state variable and provide proxies of its return rate to equilibrium after a perturbation. Ecosystems close to a transition have state variables with decreased equilibrium return rates following perturbations [10]. These state variables also are increasingly temporally autocorrelated and show high variability [10]. Therefore, autocorrelation [11,12], and standard deviation [13] are both expected to increase as resilience is lost prior to a transition. In some cases, disturbances push the state of an ecosystem toward near-tipping-point values, and therefore, the distribution of the time series also becomes asymmetric [5]. Under such situations, we may observe a rise in the skewness of the time series [1]. Alternatively, a general model may be fitted to a state variable that can approximate non-linear processes (e.g., Nonparametric Drift Diffusion Jump—NDDJ—model) [10].

Despite the strong theoretical underpinning that supports these ideas [11], evidence from empirical demonstrations is limited and real-world tests are rare [12]. One important reason is that most of the metrics require high-frequency observations of relevant environmental variables. Lack of such observations imposes limitations because, in practice, it is difficult to measure high-frequency time series of the right variables at the appropriate scale. For instance, the data to explore the state of an ecosystem may need to be collected through long-term fieldwork [2,8,10,13]. As an alternative, remote sensing datasets with high temporal resolution may provide relevant ecosystem variables that can be used to retrieve indicators of critical transitions through time.

We expect that remote sensing can significantly improve our ability to estimate critical transitions. Firstly, the wealth of remote sensing data from many sensors, wavelengths, and resolutions can play an important role in characterizing the properties and functioning of complex ecosystems and their processes. Secondly, the repeated and consistent observations of the Earth's surface by remote sensing across large spatial extents makes these data ideal for monitoring ecosystem dynamics and evaluating inter-annual variability, magnitudes, and changes of associated ecosystem processes. Although remote sensing data can be used to characterize ecosystem variables, it is not known whether spectral data are suitable to estimate critical transitions in complex ecosystems. Moreover, remotely sensed spectral data are not equally sensitive to changing conditions in an ecosystem, and time series of some variables cannot provide a timely warning of critical transitions [14]. Therefore, testing the potential of remotely sensed variables to quantify ecosystem resilience is crucially needed [14,15]. For example, it has been shown that time series of NOAA-AVHRR Normalized Difference Vegetation Indices (NDVI) provides valuable information about the functioning, state, and variability of a wetland ecosystem at global and regional scales [16]. In addition to NDVI, other spectral indices, such as the Modified Normalized Difference Water Index (MNDWI), which provides information on water extent, can be related directly or indirectly to the status of a wetland ecosystem [17].

This study tested if remote sensing data can estimate critical transitions in a wetland ecosystem. It is based on two wetland ecosystems in Iran and Armenia: one that has faced rapid algal blooming in

the last decade due to eutrophication stress (Dorge Sangi in Iran), and one that is located in a protected national park that has not experienced a serious change or a regime shift (Lake Arpi in Armenia), used as a case control. We hypothesize that a combination of water and vegetation indices can be applied to represent the state of a wetland ecosystem and estimate critical transitions. Besides existing indices, we propose a new composite index and test whether it can enhance the ability of leading indicators to generate early warning signals of a critical transition in a wetland ecosystem.

2. Materials and Methods

2.1. Study Sites

Dorge Sangi is a wetland with fresh to brackish water covering an area of 380 hectares, lying in a closed basin in the northwest of Iran (36°59.4′N, 45°33.6′E) and in the south part of lake Urmia (the sixth largest Salt Lake in the world; Figure 1B). It is a shallow wetland where the water table fluctuates according to seasonal precipitation. In the study area, the wet season is in winter, when most precipitation falls, and the dry season is in summer. The wetland was designated as a Ramsar Site (Convention on Wetlands of International Importance) in 1975 given its rich biodiversity and importance as a bird sanctuary, particularly for migratory water birds [18].
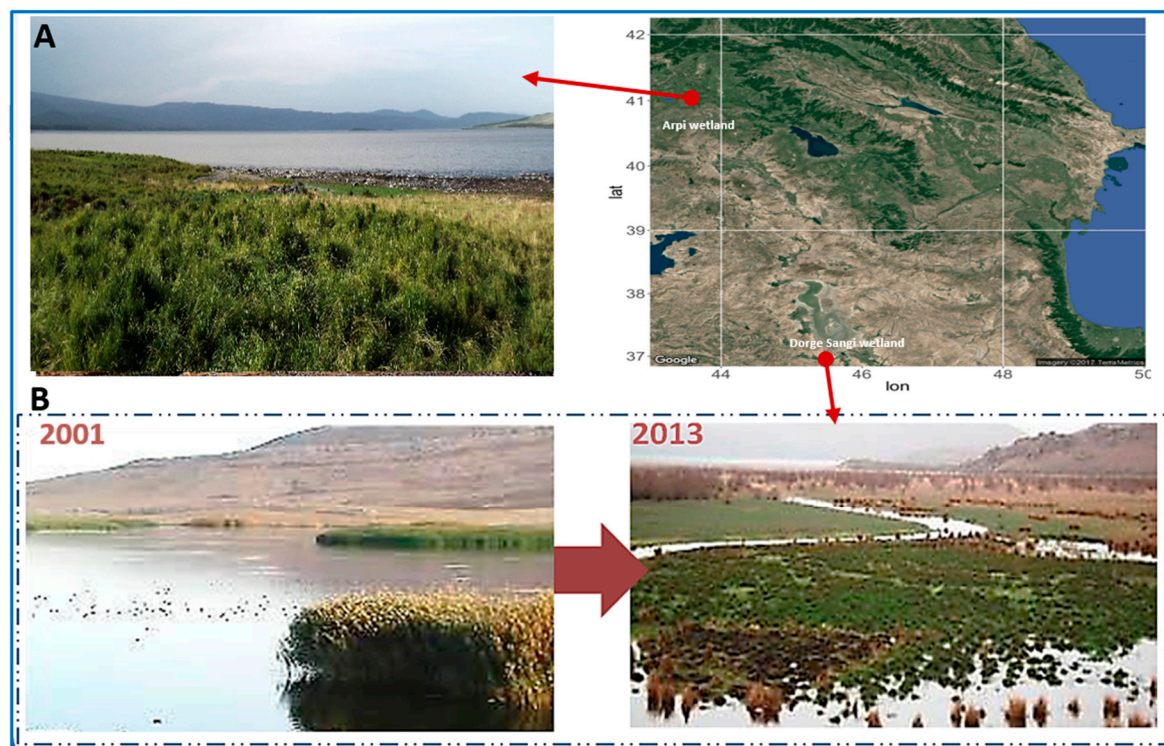

Figure 1. Location of the two case studies: (**A**) Lake Arpi in Armenia in August 2014; (**B**) The Dorge Sangi wetland in Iran; the two photos represent the condition of the study area in the spring time of the years 2001 and 2013.

The water level in Dorge Sangi has been influenced by the drastic changes in the water level of Lake Urmia, located in the northern border of the study area. Decreases in the extent of Lake Urmia to about 10% of its original size in the last decade have been reported [19,20] as a critical transition toward an alternative state—a salt pan—which is similar to the catastrophic death of the Aral Sea [21]. The variation of the water level in Lake Urmia, derived from Satellite Radar Altimetry data of Jason-3, Jason-1 and TOPEX/P [22] (Figure 2A), shows that this ecosystem dried completely around 2010, and water level fluctuations were lost afterward. The water body in Dorge Sangi displayed serious

reduction in both water level and hydroperiods starting in 2003 [23]. The reduction hits a peak in 2006 and lasted until 2013. These changes were the result of regional water resource development plans. These water level reductions were intensified by an increase in the frequency and severity of droughts. To demonstrate the regional decrease in precipitation, Figure 2B displays the standard precipitation index (SPI). The SPI is a meteorological drought index, recommended by the World Meteorological Organization and measures normalized anomalies in precipitation [24].
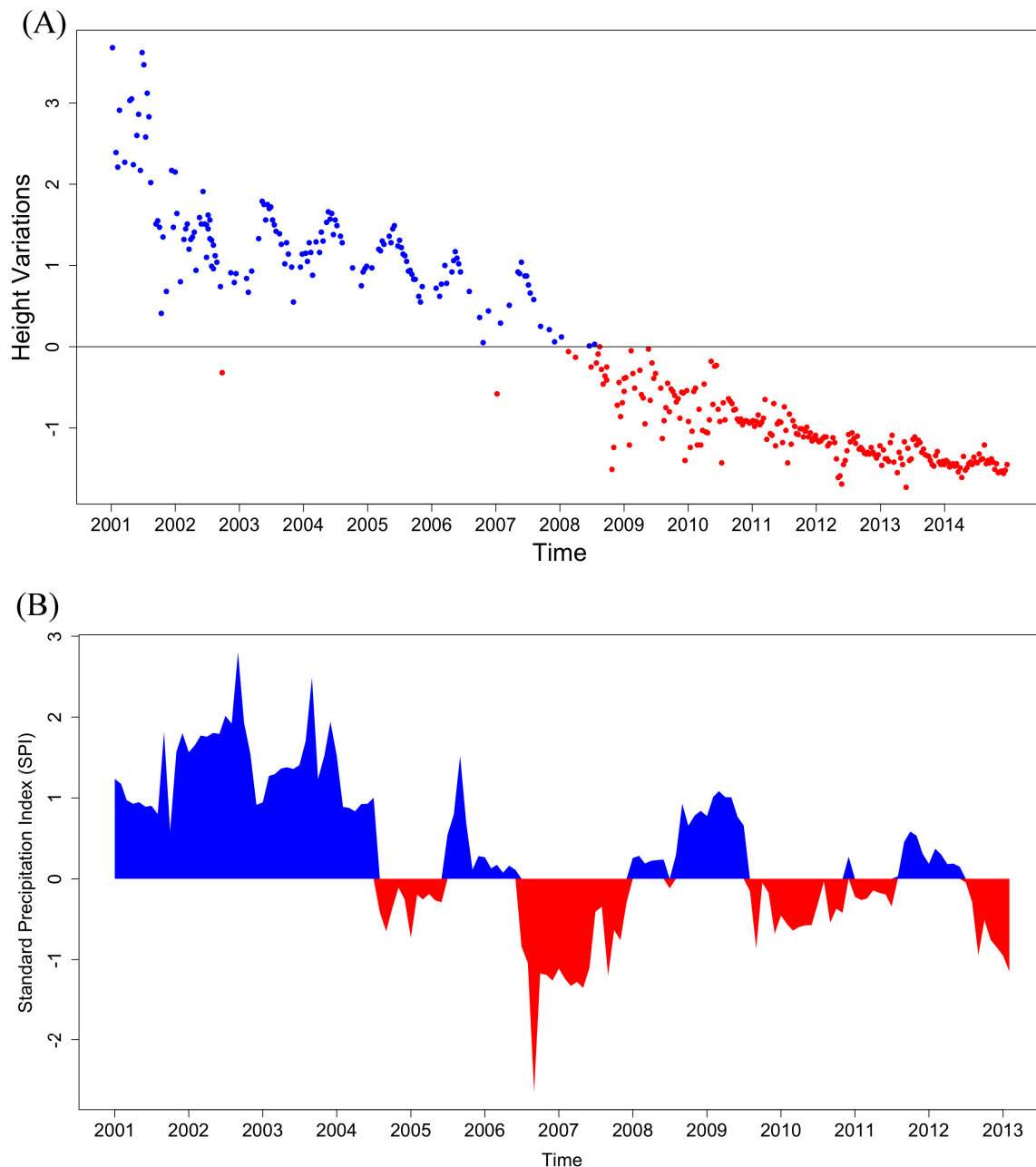

Figure 2. Urmia Lake height variation (in meters) for years 2001–2014 based on satellite radar altimetry data (**A**); Standard Precipitation Index (SPI) for Dorge Sangi during, years 2001–2013, based on measurements from Naghadeh, which is the nearest weather station to Dorge Sangi (**B**).

The drought periods were not the only reason for reductions in the hydroperiods of the basin [21,23]; the over-use of water wells, instead of using surface water runoff, and filling of surface water canals with sediments (which cut off water flow to the wetlands) led to even further reductions in

the water balance of the ecosystem and water level fluctuations. Water level fluctuations may be one of the reasons for the regime shift in Dorge Sangi, as it has negative impacts on species richness [25], and aquatic habitats [26]. In addition, it can create stressed conditions to which only specialized vegetation is adapted [27], that, in turn, changes the dynamics of vegetation in wetlands [28]. Studies also showed that changes in water quality and quantity may result in a large shift in plant communities and change the trophic state of a wetland [29]. Moreover, the observed elevation in salinity (from 0 up to 20 ppt in our study period) and nutrient loading [30] in Dorge Sangi, as a result of rising agricultural activities, created favorable conditions for blue-green algae blooms [30,31]. In addition, a complete drought was reported in Dorge Sangi in 2011, that was probably because of the construction of a new water drainage channel [30]. All of these changes have resulted in the Dorge Sangi site being included in the international Montreux Record—a list of wetland sites where major changes in ecological properties are occurring or are expected to occur—in 2007.

Our second study site is a wetland considered to be of international importance on the Ramsar list in Armenia, called Lake Arpi (located 41°03′N 43°37′E) in the Lake Arpi National Park. It has an almost similar eco-hydrological system as Dorge Sangi, consisting of fresh water with less than 100 cm depth similar to Dorge Sangi prior to the disturbances. Both wetlands are mainly fed by precipitation and are listed in the Ramsar convention. The mean annual temperature in Dorge Sangi is 12.1 °C and in Arpi 11 °C; and the mean annual precipitation in Dorge Sangi is 471 mm and in Arpi 550 mm. As the Arpi wetland is located in a protected national park, it has been undisturbed by anthropogenic effects. This healthy wetland ecosystem will be used as a case-control for validating the results.

2.2. Remote Sensing Data

2.2.1. MODIS Data

Moderate-Resolution Imaging Spectroradiometer (MODIS) surface reflectance products (MOD09A1 V5 at 500 m resolution) were downloaded from NASA Land Processes Distributed Active Archive Center; LP DAAC as eight-day composites from January 2001 to December 2014. The Dorge Sangi and Arpi study sites comprised 15 and 35 MOD09A1 pixels, respectively, that remained constant for the entire period from 2001 to 2014. A pixel was designated as a wetland pixel based on the national map of land cover of Iran with a Landsat resolution (i.e., 30 m [32]) for Dorge Sangi, and on the visually delineated wetland boundary from Landsat image of Arpi in 2014.

Each surface reflectance (MOD09A1) pixel contains the best possible L2G observation during an eight-day period (e.g., no clouds or cloud shadow and low aerosol loading). These data were used to calculate the vegetation and water spectral indices (explained in the following sub-sections). The time series of the spectral indices were then aggregated using a mean function for each month at each pixel. To estimate the overall changes for each study area, the pixels were then spatially aggregated also using a mean function into a single value for each month. We used the quality flag layer of the image product to remove poor quality retrievals, and applied a linear interpolation method to fill in the gaps in the time series. We used monthly data in this study for two reasons: (1) previous studies have shown that both gradual and abrupt changes in wetlands can be appropriately quantified at a monthly temporal resolution [16,33,34]; and (2) it was the optimum temporal resolution which minimized missing values (i.e., maximized the number of best quality surface reflectance retrievals) throughout the time series.

2.2.2. Spectral Indices

We used the 'golden standard' in vegetation monitoring, Normalized Difference Vegetation Index (*NDVI*), because it is the most widely used vegetation spectral index and is also provided as a long time-series for the entire world. It can be particularly useful for indicating nutrient levels, as well as

assessing eutrophication in wetlands [35,36], and therefore, it might characterize a critical transition in the chemical state of wetlands [37]. *NDVI* was calculated as [38]:

$$NDVI = \frac{B_{nir} - B_{red}}{B_{nir} + B_{red}} \quad (1)$$

where B_{red} and B_{nir} are the surface reflectance factors in the red MODIS band (band 1, 0.620 to 0.670 μm) and the near infrared (NIR) MODIS band (band 2, 0.841 to 0.876 μm), respectively. Higher values of *NDVI* indicate more green vegetation.

In addition, we used a water index, *MNDWI*, that can be used to delineate surface water features and estimate the amount of water in an ecosystem [39]. *MNDWI* was reported as the most reliable index among 11 remotely sensed water indices [40–42] to generate reliable information from MODIS images [43,44]. *MNDWI* was calculated as:

$$MNDWI = \frac{B_{Green} - B_{SWIR}}{B_{Green} + B_{SWIR}} \quad (2)$$

where B_{SWIR} refers to the surface reflectance of shortwave infrared (SWIR) MODIS band (band 6, 1.23 to 1.25 μm), and B_{Green} refers to green MODIS band (band 4, 0.55 to 0.57 μm).

In addition, we propose a new index, the Modified Vegetation Water Ratio (*MVWR*), which is the ratio of vegetation cover to open water cover. It uses the information content of four spectral bands (green, red, NIR and SWIR), and therefore, it potentially contains more information about the wetland's physical status. It has been argued that an index based on combining vegetation and water may reflect a wetland ecosystem functioning more efficiently than either vegetation or water index alone [45]. The new index we propose is based on an existing composite index called the Vegetation Water Ratio (*VWR*). *VWR* was put forward based on simply applying the ratio of a vegetation index (e.g., *NDVI*) to a water index, called Land Surface Water Index (*LSWI*). *LSWI* has been shown to successfully estimate the successional stages in a wetland ecosystem [45]. Thus, *VWR* can be calculated as:

$$VWR = \frac{\sum NDVI}{\sum LSWI} \quad (3)$$

where $\sum NDVI$ and $\sum LSWI$ are the annual sums of *NDVI* and *LSWI*, respectively. In order to have *VWR* comparable with the other indices, we used the monthly sums of *NDVI* and *LWSI* in this study. *LWSI* is positively correlated with the cover of water in a pixel, and is calculated as:

$$LSWI = \frac{B_{nir} - B_{SWIR}}{B_{nir} + B_{SWIR}} \quad (4)$$

where B_{nir} and B_{SWIR} are the surface reflectance factors of corresponding MODIS bands.

Inspired by this, we propose our new index *MVWR* based on the ratio of rescaled *NDVI* and *MNDWI* indices calculated on a monthly basis as:

$$MVWR = ln\left(\frac{NDVI + 1}{MNDWI + 1}\right) \quad (5)$$

We calculated *MVWR* on a monthly basis, as leading indicators need a high temporal resolution, and a monthly time step was also used for *NDVI* and *MNDWI*. As *NDVI* and *MNDWI* roughly range between −1 and +1, we simply rescaled them to a range between 0 and 1 to avoid the effect of negative values in the composite index. We scaled the indices by adding a value of +1 to each index, and then dividing it by 2. In the calculation of the ratio, the division term is lost. We smoothed the time series of *NDVI* and *MNDWI* using a moving average (a symmetric window with a size of 3 and equal weights) prior to the calculation of the index. *MVWR* indicates more green cover at positive values, and more water cover at negative values. We selected *MNDWI* instead of the *LSWI* to calculate the *MVWR*

because it has been shown in a number of studies that *MNDWI* is a more reliable index compared to other water indices including *LSWI* [41,42,46].

2.3. Leading Indicators for Critical Transition

A recently suggested approach to generate early warning measures of critical transitions is to use statistics that measure the critical slowing down in the dynamics of a state variable of a system as a transition is approached [10,47–49]. This slowing down is the result of decreases in the rates of recovery in a system after perturbations [7,50].

We used two kinds of indicators: metric-based and model-based indicators [51]. Metric-based indicators quantify changes in the statistical properties of a time series—including autocorrelation, standard deviation, and skewness—without fitting data to a specific model structure. Model-based indicators, attempt to fit a model to data in order to quantify the changes [51]. In the case of a noisy time series, Nonparametric Drift Diffusion Jump (NDDJ) models can be used for this. Both types of indicators try to capture changes in the correlation structure and variability of a time series.

All analyses were implemented in the R environment v. 3.3.1 [52] using functionalities of the rts package for manipulating time series of satellite images [53], and the early warnings package for calculating the leading indicators [5].

2.3.1. Metric-Based Indicators

Critical transitions can be expressed in a time series of a state variable in a system using several metric-based indicators: autocorrelation [54,55], variance [10], and skewness [1]. Analysis of simulation models exposed to stochastic forcing showed that if the system is driven gradually closer to a tipping point, there is a marked increase in the autocorrelation that builds up long before the critical transition occurs [1]. An increase in autocorrelation indicates that the state of a system becomes more similar between consecutive observations [11], and can be considered as the simplest way to measure critical slowing down [56]. Autocorrelation can be calculated considering a certain time lag. Most studies on leading indicators so far have considered time lags of one time-step, or lag-1 autocorrelation. We followed the same rule. It can be calculated by [11]:

$$\rho_1 = \frac{E[(z_t - \mu)(z_{t+1} - \mu)]}{\delta_z^2} \tag{6}$$

where μ is the mean and δ is the variance of variable z_t.

Slow return rates to a stable state can also make the system drift wider around that state, and cause increased variance in the fluctuations prior to a transition [1,11]. Variance is the second moment around the mean of a distribution and can be expressed as standard deviation by:

$$SD = \sqrt{\frac{1}{n-1}\sum_{t=1}^{n}(z_t - \mu)^2} \tag{7}$$

In addition to autocorrelation and variance, an increase in the asymmetry of fluctuations may happen as a result of an unstable equilibrium close to a tipping point [1]. In such cases, we can observe a rise in skewness [5]. Skewness is the standardized third moment around the mean of a distribution and can be calculated by [1]:

$$SK = \frac{\frac{1}{n}\sum_{t=1}^{n}(z_t - \mu)^3}{\sqrt{\frac{1}{n}\sum_{t=1}^{n}(z_t - \mu)^2}} \tag{8}$$

Before applying the metric based models, the data should be detrended and smoothed to eliminate the effect of nonstationary conditions on the leading indicators. Several detrending approaches are commonly used including Gaussian, Linear and Loess filters, and first-differencing [57]. Filtering methods detrend within a rolling window [11]. We used Kendall's τ between each indicator and time

to find the best size of the rolling window and the best bandwidth (for the Gaussian filter) through a sensitivity analysis. Kendall's τ is a nonparametric statistic to measure the association between two measured quantities [58] ranging from −1 to +1. Greater Kendall's τ values refer to stronger trends [58]. We tried to identify those detrending settings that best identify trends in leading indicators. Thus, we calculated the leading indicators for various sizes of rolling windows (ranging from 25% to 75% of the time series length) and bandwidths (ranging from 25% to 75% of the time series length for the Gaussian filter) with increments of 10% for four different detrending approaches (Gaussian, loess, and linear filters, and first-differencing).

We also tested whether the trends in the leading indicators were not due to random chance. To do so, 1000 surrogate datasets were generated by fitting the best linear autoregressive moving average model (ARMA) based on AIC to the residuals after detrending with the same length as the residual time series [5]. Following [5], the trend estimations from the original data were compared with the trend estimations from the surrogate data with the same correlation structure and probability distribution as the original dataset. For each simulated dataset, we estimated the trend in autocorrelation, skewness, and standard deviation using Kendall's τ. We then estimated the probability of finding a trend by chance by comparing Kendall's τ of the original data to the number of cases in which the statistic was equal to or smaller than of the estimates of the simulated records, $P(\tau^* \leq \tau)$. Trends were calculated over the entire time series, except when there was a clear break point, in which case tau was calculated for the part of the time series before the break point occurred.

2.3.2. Model-Based Indicators

Metric-based indicators have a risk of showing false signals of upcoming critical transitions given their sensitivity to the size of rolling window and detrending method [5]. Although we tried to find the best settings for these parameters through the sensitivity analysis, we also used the model-based indicators using the NDDJ model, that can identify a critical transition without the need to specify a rolling window and detrending of the data [10]. The equation to estimate the NDDJ model is:

$$dx_t = \mu(x_{t-}, \theta_t)d_t + \sigma_D(x_{t-}, \theta_t)dW + d\left(\sum_{n=1}^{N_t} Z_n\right) \tag{9}$$

where the drift term $\mu(x_{t-}, \theta_t)$ measures the instantaneous deterministic change in the time series, the diffusion term $\sigma_D(x_{t-}, \theta_t)$ measures the standard deviation of relatively small shocks that occur at each time step, and the jumps (the last term in Equation (9)), are relatively large shocks that occur intermittently. Jumps are characterized by an average magnitude $\sigma_Z(\theta_t)$ where $Zn \sim N(0, \theta_t)$, and the probability of a jump arriving in a small time increment (i.e., d_t) is $\lambda(x_{t-}, \theta_t) d_t$. The subscript t-indicates that a function is evaluated just before each time step. Total variance combines the contributions of diffusion and jumps together [59–61].

The outputs of this model can signal an upcoming critical transition in several ways [5,60], including: (1) an increase in the trends of drift and diffusion; (2) an increase in the total variance (which is based on the composition of the diffusion and jump variance, shown to detect a critical transition with high precision by [60]; (3) an increase in the conditional variance of x (which is estimated as the difference between the second conditional moment and the square of the first conditional moment; see [5] for the details); (4) an increase in the jump intensity; and (5) increased fluctuations of the total variance and the jump intensity between their maximum and minimum values.

3. Results

3.1. Detecting Critical Transition

We started our analysis by examining the spectral behavior of the two study sites at the beginning and the end of the time series (i.e., the years 2001 and 2014) in the wet and dry seasons (i.e., January, and August respectively; Figure 3). This shows whether the spectral profile changed before and after the transition. In Dorge Sangi, a large difference can be observed in the spectral profiles of the years 2001 and 2014 for both the wet and dry seasons, suggesting changes in the area between the two years. In contrast, the mean surface reflectance factors in the healthy Arpi wetland showed similar behavior between the two years for the wet and dry season. The overall level of the surface reflectance factors in Arpi was also higher than in Dorge Sangi.
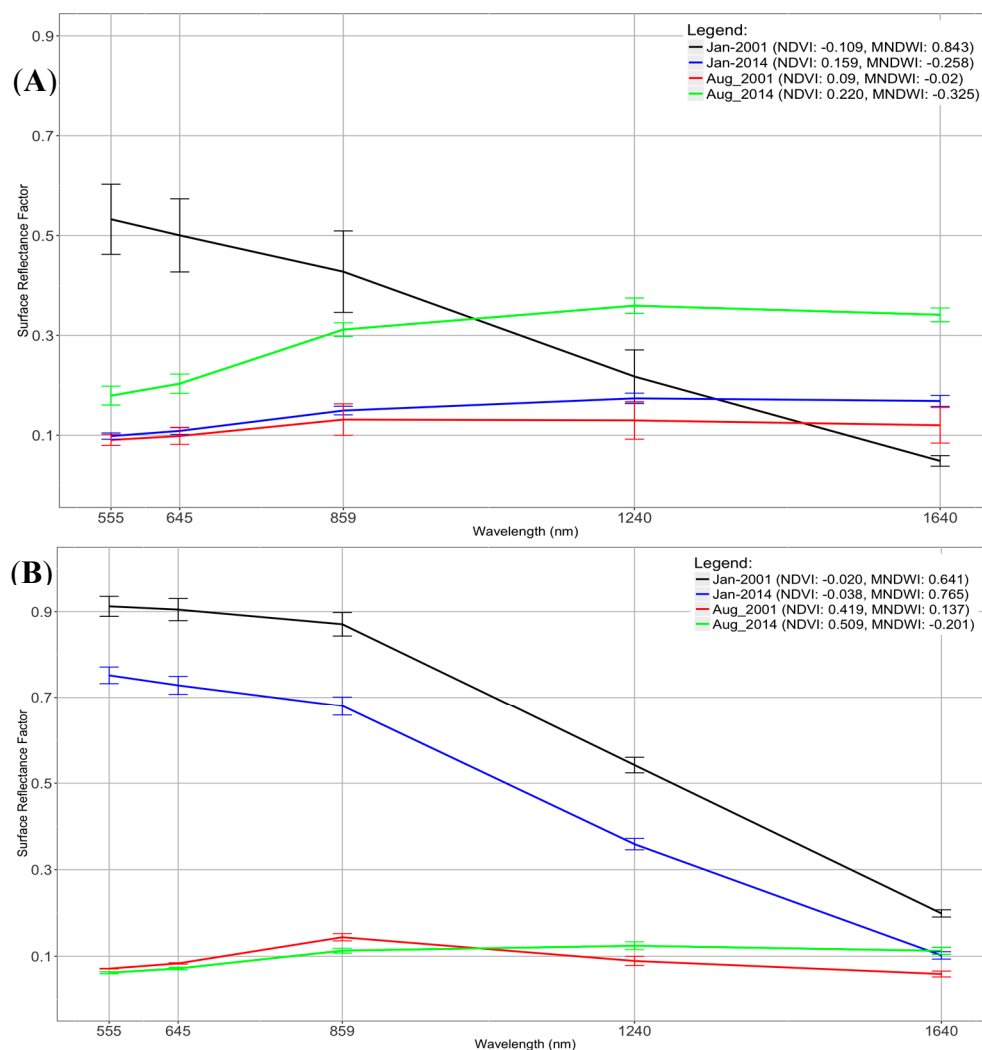

Figure 3. Mean spectra in Dorge Sangi wetland (**A**) and Arpi wetland (**B**) from Moderate-Resolution Imaging Spectroradiometer (MODIS) satellite images (MOD9A1 product) of the five spectral bands (bands 1, 2, 4, 5, and 6) that have been used to calculate the spectral indices in this study. Bars show the standard errors over different pixels in the study area. Different colors show the profiles for two different seasons at the beginning and end of the time series.

The seasonal fluctuations during the study period can be recognized in the time series of all the indices (Figure 4) and these patterns are much more regular in the undisturbed system (Arpi) than in the disturbed system (Dorge Sangi). Moreover, an abrupt increase in *NDVI* and *MVWR*, and an abrupt decrease in *MNDWI* can be noticed for Dorge Sangi in 2009. In the Arpi wetland, only slight variations over time can be seen and no significant trend is noticeable. This suggests that the spectral indices in the healthy Arpi wetland remained consistent throughout the study period.
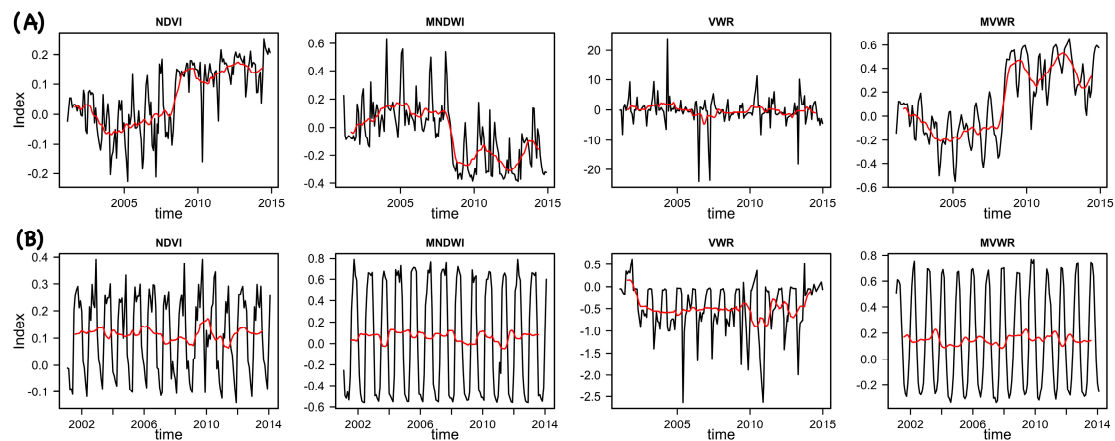

Figure 4. The time series of four remotely sensed indices, Normalized Difference Vegetation Index (*NDVI*), Modified Normalized Water Index (*MNDWI*), Vegetation-Water Ratio (*VWR*), and Modified Vegetation-Water Ratio (*MVWR*) used as the variables in (**A**) Dorge Sangi study site, and (**B**) Arpi study site. The red line indicates the trend obtained using a moving average with a window size of 3 time steps.

3.1.1. Metric-Based Indicators

The first-difference detrending method resulted in the strongest trends, as expressed by Kendall's τ at a rolling window size of around 50% of the time series, for most indices. This rolling window should not be either too short, as that can lead to noisy time series, or too long, as that smoothes the fluctuations that may be indicative of a critical transition. The sensitivity analysis on the trends in the leading indicators show that autocorrelation of *MVWR* and *MNDWI* is less sensitive to the rolling window size than the other indices (Figure 5). The positive Kendall's τ for *MVWR* obtained from all indicators (around 0.9 for both the skewness and autocorrelation, and around 0.5 for the standard deviation) suggests that the leading indicators based on this spectral index correlated the strongest with the observed critical transition in the wetland, compared to *NDVI*, *VWR*, and *MNDWI*. In Arpi, all the indices showed less sensitivity to the sizes of the rolling window, except *VWR* that showed sensitivity for the Skewness.

The probability of whether significant positive trends of the indicators detected in the spectral indices are due to chance (based on the comparison with the surrogate datasets) was very low for all the indicators and across all the indices (Table 1). This suggests that the significant positive trends found in the original datasets relate to the described critical transition.
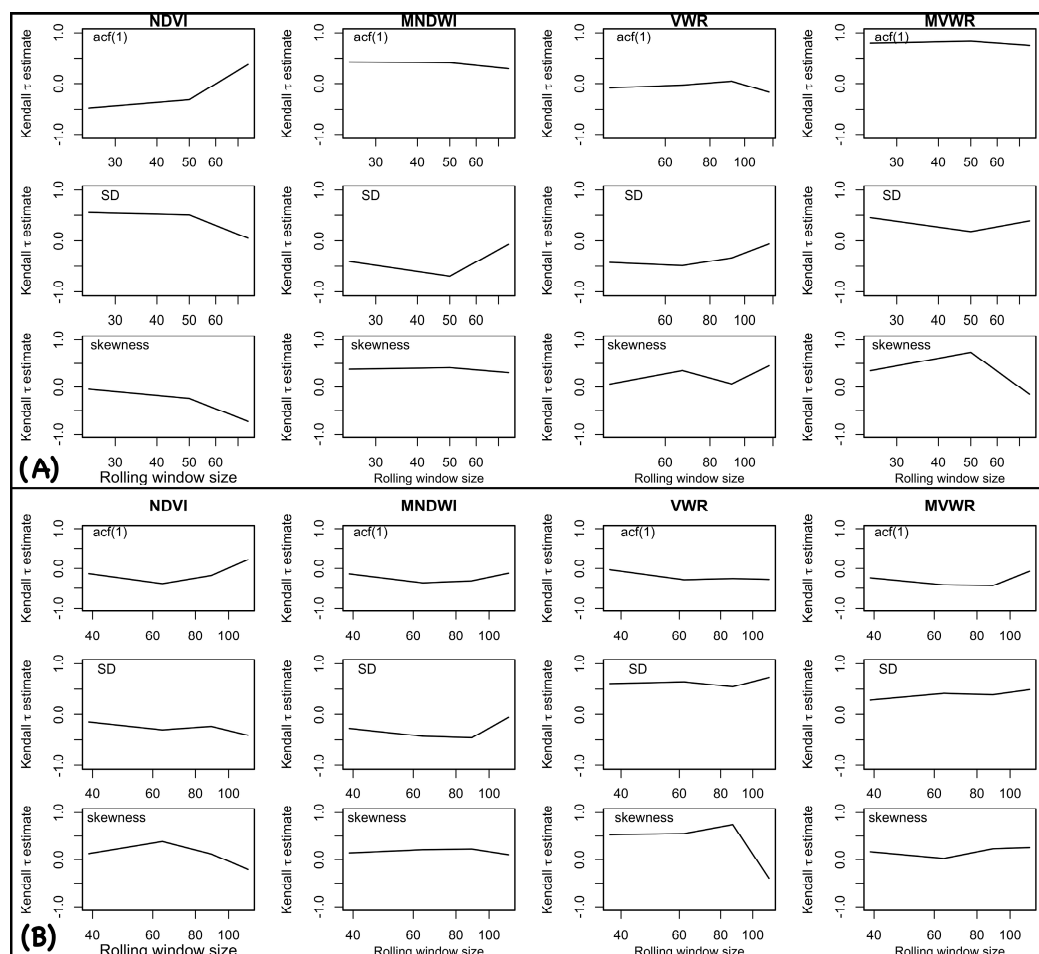
Figure 5. Sensitivity analysis of metric-based indicators to rolling window size given the first-differential filter for different spectral indices (columns). First, second, and third rows show autocorrelation at lag-1, standard deviation, and skewness, respectively for the Dorge Sangi (**A**), and Arpi (**B**) study sites.

Table 1. Kendall's τ trend and its associated significance (Dorge Sangi | Arpi).

Spectral Indices	Indicators		
	Autocorrelation	**Standard Deviation**	**Skewness**
NDVI	0.296 * | −0.293 ***	−0.514 *** | −0.389 ***	0.439 * | −0.409 ***
MNDWI	0.397 *** | −0.268 ***	−0.782 *** | −0.499 ***	0.127 *** | 0.275
VWR	0.152 | 0.019	−0.523 *** | 0.698 ***	0.145 | −0.633
MVWR	0.850 *** | −0.225 ***	0.406 *** | 0.285 ***	0.754 *** | −0.025 ***

Significance level: *** $P < 0.001$; ** $P < 0.01$; * $P < 0.05$, $P < 0.1$.

In Dorge Sangi, *MVWR* showed a strong significant increase in the autocorrelation (Figure 6A, Kendall's τ = 0.850) before September 2009, and a strong significant decrease (Kendall's τ = −0.812) after that time. This could be indicative of a critical transition [6,12,62,63] with a tipping point at the time of the change in trend (i.e., September 2009). The positive trend prior to the transition suggests that the ecosystem slowed down, acting as an early warning signal for the transition. The negative trend after the tipping point suggests that the ecosystem stabilized at a new state after the transition. Autocorrelation in *MNDWI* and *NDVI* mirrored the observed pattern in *MVWR*, but had a lower magnitude and were more erratic than *MVWR*. *NDVI* and *MNDWI* showed a negative trend in the standard deviation and therefore does not act as a warning signal of the critical transition. In contrast, the standard deviation of *MVWR* showed a positive trend in the first years of the time series, but

this trend extended beyond the moment the system switched and only started declining after 2012. Similarly, the skewness of *MNDWI* showed a positive trend prior to the transition in Dorge Sangi, followed by a negative trend, but here the signal also switched sign in 2012 rather than 2009. In addition, *MVWR* was the only variable that showed a positive trend for all the indicators and the strongest trend for most of the indicators in Dorge Sangi (Figure 6A and Table 1).
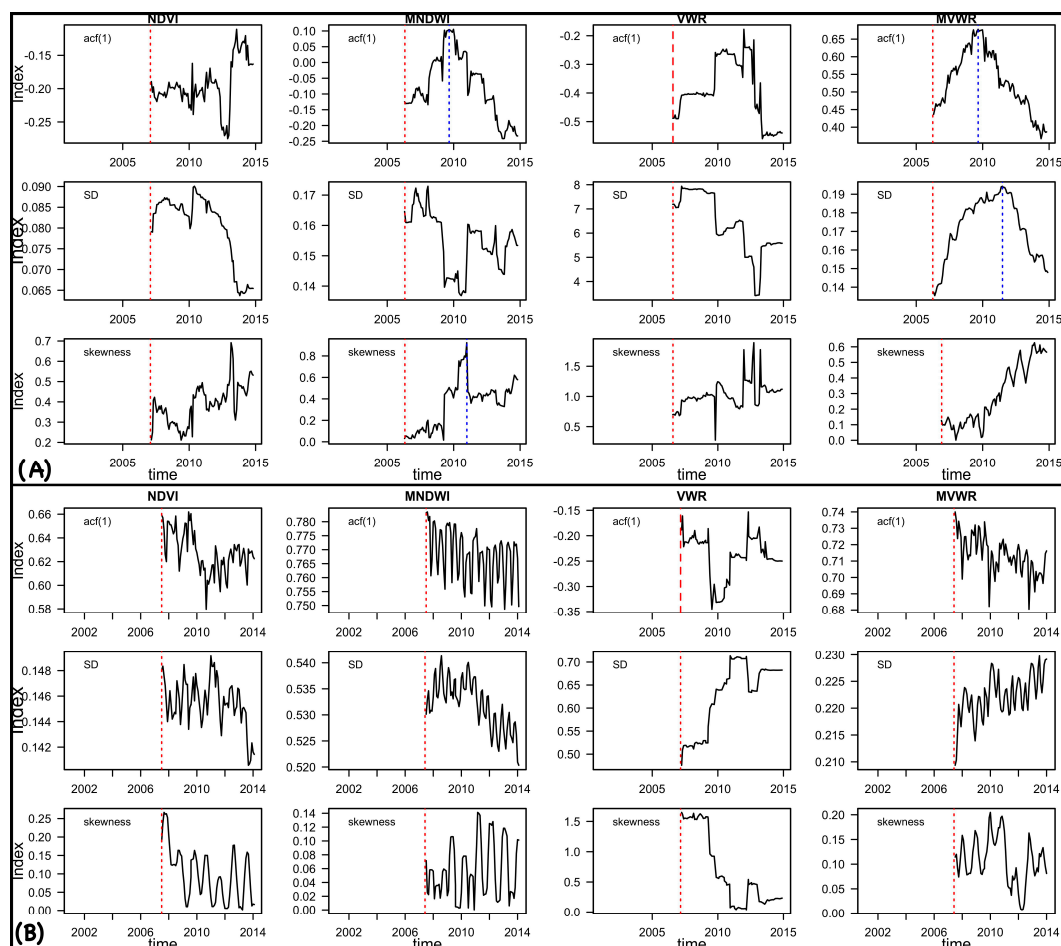

Figure 6. Metric-based leading indicators based on *NDVI*, *MNDWI*, *VWR*, and *MVWR* for Dorge Sangi (**A**), and Arpi (**B**) wetlands. The first, second, and third rows show autocorrelation at lag 1 (acf), standard deviation (SD), and skewness of each spectral indices, respectively; the red dotted lines mark the width of the rolling window used to detrend the data; the blue dotted lines mark the moment the trend changes abruptly which could be indicative of a tipping point.

VWR showed a clear jump in the autocorrelation at the moment of the transition. However, similar jumps can be noticed at the other moments where no transition was supposed to happen, making indicators based on this index less reliable.

The results from Arpi showed no evidence of transitions from the different spectral indices (Figure 6B) although some sudden jumps can be observed in the indicators based on *VWR*, reconfirming the erratic nature of the indicators based on this index. These results showed a significant trend in the standard deviation of *VWR* as well as a weak but significant increase in the standard deviation of *MVWR*. Given the known history of Arpi as a healthy wetland, these positive trends can be considered as false alarms.

3.1.2. Model-Based Indicators

The model-based indicators showed clear differences before and after the transition that happened in Dorge Sangi in 2009 (Figure 7A). We can see an increase in the total variance and jump intensity of *NDVI*, and *MNDWI* between 2004 and 2009. In addition, the total variance of *MVWR* increased after 2004, while it switched from positive spikes to negative spikes after 2009. Furthermore, the diffusion values for *MVWR* fluctuated between their maximum and minimum values up to 2009 but fluctuations subdued after 2009. All these sudden changes in the signal are probably an indication of the transition that happened in 2009. Moreover, it seems that the signals act as the early warnings of the impending shift started from 2004.
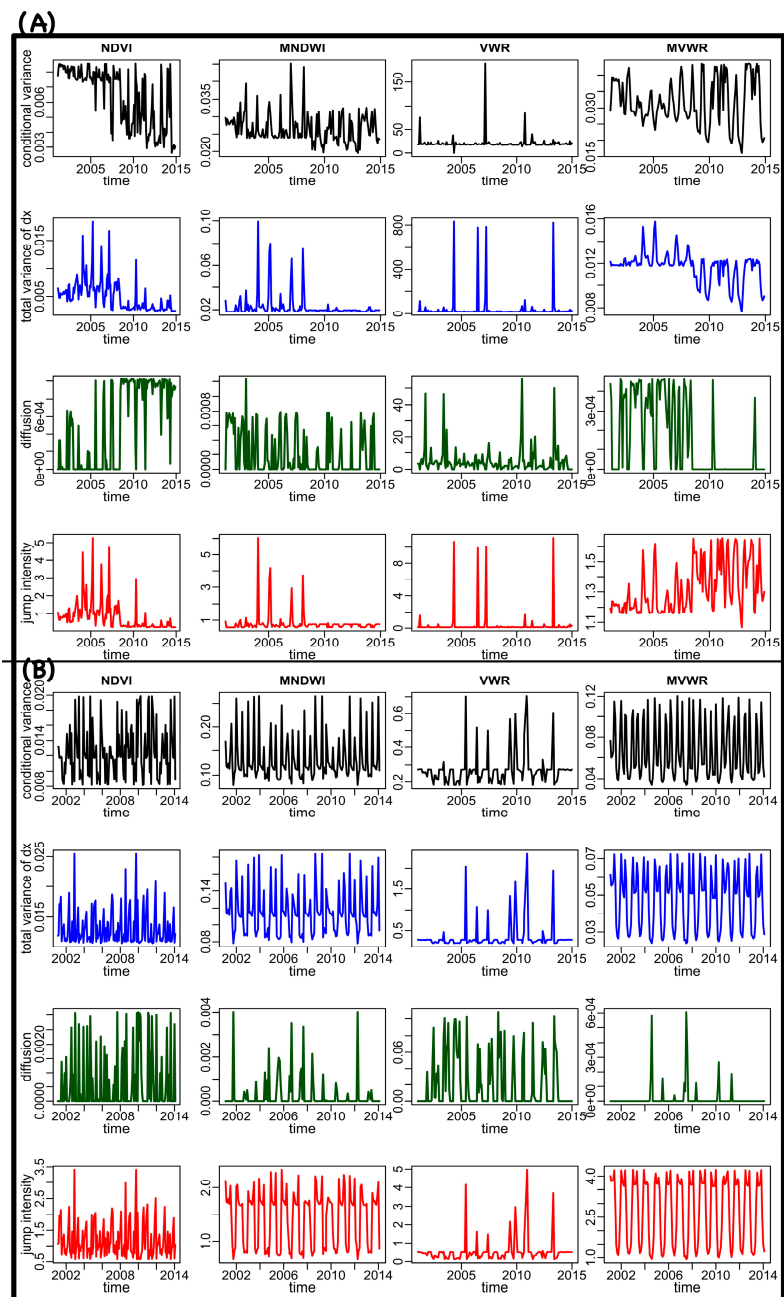

Figure 7. Nonparametric drift diffusion jump model of the monitored spectral indices *NDVI*, *MNDWI*, *VWR*, and *MVWR* versus time in the study sites Dorge Sangi (**A**), and Arpi (**B**).

For the healthy system, no clear sudden changes in patterns can be observed (Figure 7B), although *VWR* is showing a rather erratic pattern, and also the diffusion indicator is not stable for *MNDWI* and *MVWR*.

4. Discussion

It has been argued that estimation of critical transitions in complex real ecosystems is difficult [64]. For example, the indicators that have been introduced for generating early warning signals may indicate a false alarm due to changes in a stochastic regime of perturbations rather than the actual ecosystem dynamics [1,47], or, most importantly, due to having insufficient or imprecise data. Although the potential of remote sensing to overcome such difficulties has been frequently acknowledged [47,65,66], its application for these purposes has rarely been tested, e.g., [67]. In this paper, we explored the performance of remote sensing data to evaluate whether robust early warning signals of a critical transition in a real-world wetland ecosystem can be derived using recently developed leading indicators.

Most of the indicators to detect critical transitions have been derived from simple models, and tested through controlled experiments [1]. Although the indicators have been well recognized in theory, demonstration of these approaches in real ecosystems has been very limited [1,50,51,63], and concerns exist that they may not work in in complex real ecosystems [64]. An important feature in this study is that we used two real ecosystems, one that experienced a critical transition (i.e., Dorge Sangi), and one that did not (i.e., Arpi). Evaluating the indicators for a real ecosystem where a transition has occurred is possibly the best way to test how well remote sensing based indicators are capable of detecting critical transitions in advance. It also allows testing the risk of false alarms in real situations.

Our results revealed that when the right spectral index, that represents the state of the ecosystem in a relevant way [11], is selected, some leading indicators seem to provide early warnings of impending transitions. These selected indices need to have a direct or indirect link to the underlying mechanisms that are driving the ecosystem changes. When underlying mechanisms in an ecosystem are known, we have greater clarity about which parameters caused system fragility. For instance, vegetation and water are both the key variables characterizing wetlands [45]. The index that was suggested to provide the most reliable indicator (*MVWR*) is also a combination of vegetation and water cover information.

In Dorge Sangi, changes in hydrological processes were due to decreasing the water levels in the wetland and increasing the intensity of droughts. These changes, along with an increase in the size of the agricultural areas near the wetland, resulted in an increase in nitrogen and phosphorus levels in water which, in turn benefited algal blooming and potentially increased wetland plants' chlorophyll concentrations [68]. Eutrophication also caused an increase in vegetation cover. This probably explains why *MVWR* indicate the changes in this system better than the other indices. The index is sensitive to the interaction of vegetation and water in a pixel based on four spectral regions. In the visible spectral domain (red), there is low reflectance when chlorophyll and carotene absorption by vegetation are high. The chlorophyll also reflects in the near infrared wavelengths due to scattering caused by internal leaf structure. At the same time, in near and short infrared domains, water bodies have their maximum absorption bands.

Whether the identified leading indicators truly indicated the occurrence of a critical transition in the Dorge Sangi wetland depends in part on the assumption that the transition in Dorge Sangi was a real ecosystem transition as a result of the loss of resilience, and that it happened around 2009. In 2006, national media, as well as several studies, reported serious changes in the Dorge Sangi wetland, that probably already started earlier [30]. The changes put the wetland on the Montreux list, a list of endangered wetlands with changes in ecological character, in 2007. In addition, changes in the vegetation structure, as well as drying, were reported based on sampling data in a period between November 2008 and February 2009. These reports suggest that the occurrence of the transition was somewhere around the year of 2009. In general, the occurrence of a regime shift in an aquatic ecosystem is considered a rapid phenomenon, compared other ecological systems such as for example forests [12].

Our results revealed that some indicators (especially the autocorrelation & the total variance in *MVWR*) seem to provide early warning signals prior to the occurrence of the critical transition.

According to the model-based indicators, the earliest signal was generated in the year of 2004, especially by the total variance. The metric-based methods, however, showed the signals started in 2006. These analyses were limited to the length of the time series that we used according to the availability of the satellite images. As the results by the metric-based indicators depend on the size of the rolling window, generating earlier signals was not possible by these methods. It might be a possibility to generate earlier signals and consequently improve the ability of anticipating the critical transition if a longer time series dataset was available.

The performance of leading indicators in identifying a critical transition is dependent on the dynamic of changes in the key ecosystem variables. In Dorge Sangi, the time series of both *NDVI* and *MNDWI* (Figure 4A) show an increase in their fluctuations prior to the abrupt change in 2009. These fluctuations are to a lesser extent also captured by the jump intensity. Our results showed agreement with other studies, e.g., [60], which mention that total variance can detect the critical transition with high precision. Along with the total variance, the autocorrelation was the metric that showed the best performance in our study and can be recommended for the other studies.

Our results showed that not all indicators that have been identified by theoretical studies seem to work in reality. For example, the trends of autocorrelation and skewness for NDVI were positive but the standard deviation showed a negative trend in Dorge Sangi. Also, we found a false alarm in the positive trend in the standard deviation of *MVWR* in the healthy Arpi wetland. Two main reasons can be discussed related to this issue. First the robustness of calculated indicators might be variable, depending on the used detrending method and the rolling window size used. Second, the ability of indices to present the state of the ecosystem can vary, depending on the form of changes in the ecosystem prior to a transition. For example, skewness only performs well when an increase in the asymmetry of fluctuations happens close to a tipping point. It has been demonstrated that while autocorrelation always increases prior to a transition, standard deviation may be underestimated as the fluctuations in an ecosystem become increasingly dominated by low frequencies close to a transition [69]. Our results showed that the best signal for the transition is based on autocorrelation compared to the other metric-based methods. It could be that these methods are more sensitive to pre-processing steps and that this affects their performance, as reported by [5].

In this study, we showed how different spectral indices from satellite data can be used to calculate leading indicators for critical transitions in an ecosystem. *MVWR* showed greater performance to identify the critical transition in the Dorge Sangi wetland comparing to the other indices. The increasing trend of *MVWR* in our case study may be due to the synergic effects of eutrophication and water stresses in the wetland.

Although there are many studies on wetlands that have used satellite images, there is a lack of studies identifying ecologically relevant dynamics such as critical transitions. To advance knowledge in this area, the present study used remote sensing data to estimate indicators for critical transition(s) in a wetland ecosystem. The integration of remote sensing with statistical approaches to estimate early warning signals of critical transitions in complex ecosystems can provide the foundation to advance significantly the characterization of ecosystem dynamics across multiple scales in space and time. Exploring the remote sensing-based metrics that have clear mechanistic links to ecosystem dynamics will facilitate the development of robust early warning systems [70] for upcoming critical transitions.

5. Conclusions

In this study, we illustrate that remotely sensed vegetation and water indices can be used to calculate indicators for critical transitions in a wetland ecosystem. We also showed that if the right spectral index is selected, temporal autocorrelation performed well in generating early warning signals and in identifying the transitions in a real-world wetland ecosystem, while other indicators mainly only identified the moment of the transition. We proposed a modified composite vegetation-water

index, *MVWR*, and demonstrated that it improved the ability to detect a critical transition in wetland ecosystems timely manner compared to either vegetation (*NDVI*), water (*MNDWI*), or existing composite vegetation-water (*VWR*) indices.

Our results demonstrate the applicability of remotely sensed metrics, particularly those that have a mechanistic link to underlying processes in an ecosystem, for exploring the state of the ecosystem and consequently improving the ability of the indicators to generate warnings of impending transitions.

Author Contributions: Sara Alibakhshi and Babak Naimi conceived and designed the project; Sara Alibakhshi executed analyses; Sara Alibakhshi, Thomas A. Groen, Miina Rautiainen and Babak Naimi wrote the paper.

Conflicts of Interest: The authors declare no conflict of interest. The funding sponsors had no role in the design of the study; in the collection, analyses, or interpretation of data; in the writing of the manuscript, and in the decision to publish the results.

References

1. Scheffer, M.; Bascompte, J.; Brock, W.A.; Brovkin, V.; Carpenter, S.R.; Dakos, V.; Held, H.; Van Nes, E.H.; Rietkerk, M.; Sugihara, G. Early-warning signals for critical transitions. *Nature* **2009**, *461*, 53–59. [CrossRef] [PubMed]

2. Bestelmeyer, B.T.; Ellison, A.M.; Fraser, W.R.; Gorman, K.B.; Holbrook, S.J.; Laney, C.M.; Ohman, M.D.; Peters, D.P.; Pillsbury, F.C.; Rassweiler, A. Analysis of abrupt transitions in ecological systems. *Ecosphere* **2011**, *2*, art129. [CrossRef]

3. Scheffer, M.; Carpenter, S.; Foley, J.A.; Folke, C.; Walker, B. Catastrophic shifts in ecosystems. *Nature* **2001**, *413*, 591–596. [CrossRef] [PubMed]

4. Brock, W.A.; Carpenter, S.R. Early warnings of regime shift when the ecosystem structure is unknown. *PLoS ONE* **2012**, *7*, e45586. [CrossRef] [PubMed]

5. Dakos, V.; Carpenter, S.R.; Brock, W.A.; Ellison, A.M.; Guttal, V.; Ives, A.R.; Kefi, S.; Livina, V.; Seekell, D.A.; van Nes, E.H. Methods for detecting early warnings of critical transitions in time series illustrated using simulated ecological data. *PLoS ONE* **2012**, *7*, e41010. [CrossRef] [PubMed]

6. Scheffer, M.; Carpenter, S.R.; Lenton, T.M.; Bascompte, J.; Brock, W.; Dakos, V.; Van De Koppel, J.; Van De Leemput, I.A.; Levin, S.A.; Van Nes, E.H. Anticipating critical transitions. *Science* **2012**, *338*, 344–348. [CrossRef] [PubMed]

7. Scheffer, M. *Critical Transitions in Nature and Society*; Princeton University Press: Princeton, NJ, USA, 2009.

8. Carpenter, S.; Brock, W.; Cole, J.; Kitchell, J.; Pace, M. Leading indicators of trophic cascades. *Ecol. Lett.* **2008**, *11*, 128–138. [CrossRef] [PubMed]

9. Scheffer, M. Complex systems: Foreseeing tipping points. *Nature* **2010**, *467*, 411–412. [CrossRef] [PubMed]

10. Carpenter, S.; Brock, W. Rising variance: A leading indicator of ecological transition. *Ecol. Lett.* **2006**, *9*, 311–318. [CrossRef] [PubMed]

11. Dakos, V.; Scheffer, M.; van Nes, E.H.; Brovkin, V.; Petoukhov, V.; Held, H. Slowing down as an early warning signal for abrupt climate change. *Proc. Natl. Acad. Sci. USA* **2008**, *105*, 14308–14312. [CrossRef] [PubMed]

12. Carpenter, S.R.; Cole, J.J.; Pace, M.L.; Batt, R.; Brock, W.; Cline, T.; Coloso, J.; Hodgson, J.R.; Kitchell, J.F.; Seekell, D.A. Early warnings of regime shifts: A whole-ecosystem experiment. *Science* **2011**, *332*, 1079–1082. [CrossRef] [PubMed]

13. Vanderploeg, H.A.; Pothoven, S.A.; Fahnenstiel, G.L.; Cavaletto, J.F.; Liebig, J.R.; Stow, C.A.; Nalepa, T.F.; Madenjian, C.P.; Bunnell, D.B. Seasonal zooplankton dynamics in lake michigan: Disentangling impacts of resource limitation, ecosystem engineering, and predation during a critical ecosystem transition. *J. Great Lakes Res.* **2012**, *38*, 336–352. [CrossRef]

14. Donangelo, R.; Fort, H.; Dakos, V.; Scheffer, M.; Van Nes, E.H. Early warnings for catastrophic shifts in ecosystems: Comparison between spatial and temporal indicators. *Int. J. Bifurc. Chaos* **2010**, *20*, 315–321. [CrossRef]

15. Lade, S.J.; Gross, T. Early warning signals for critical transitions: A generalized modeling approach. *PLoS Comput. Biol.* **2012**, *8*, e1002360. [CrossRef] [PubMed]

16. Zoffoli, M.L.; Kandus, P.; Madanes, N.; Calvo, D.H. Seasonal and interannual analysis of wetlands in south america using noaa-avhrr ndvi time series: The case of the parana delta region. *Landsc. Ecol.* **2008**, *23*, 833–848. [CrossRef]

17. Ray, R.; Mandal, S.; Dhara, A. Characterization and mapping of inland wetland: A case study on selected bils on nadia district. *Int. J. Sci. Res. Pub.* **2012**, *2*, 12.

18. Lotfi, A.; Moser, M. *Water for Ecosystems*; Ministry of Energy: Victoria, BC, Canada, 2005.

19. Asem, A.; Mohebbi, F.; Ahmadi, R. Drought in urmia lake, the largest natural habitat of brine shrimp artemia. *World Aquacult.* **2012**, *43*, 36–38.

20. Hoseinpour, M.; Fakheri Fard, A.; Naghili, R. Death of Urmia Lake, a Silent Disaster Investigating causes, results and solutions of Urmia Lake drying. In Proceedings of the 1st International Applied Geological Congress, Mashad, Iran, 26–28 April 2010; pp. 700–704.

21. AghaKouchak, A.; Norouzi, H.; Madani, K.; Mirchi, A.; Azarderakhsh, M.; Nazemi, A.; Nasrollahi, N.; Farahmand, A.; Mehran, A.; Hasanzadeh, E. Aral sea syndrome desiccates lake urmia: Call for action. *J. Great Lakes Res.* **2015**, *41*, 307–311. [CrossRef]

22. Birkett, C.; Reynolds, C.; Beckley, B.; Doorn, B. From research to operations: The usda global reservoir and lake monitor. In *Coastal Altimetry*; Springer: New York, NY, USA, 2011; pp. 19–50.

23. Hassanzadeh, E.; Zarghami, M.; Hassanzadeh, Y. Determining the main factors in declining the urmia lake level by using system dynamics modeling. *Water Resour. Manag.* **2012**, *26*, 129–145. [CrossRef]

24. McKee, T.B.; Doesken, N.J.; Kleist, J. The Relationship of Drought Frequency and Duration to Time Scales. In Proceedings of the 8th Conference on Applied Climatology, Boston, MA, USA, 17–22 January 1993; pp. 179–183.

25. Sutela, T.; Vehanen, T. Effects of water-level regulation on the nearshore fish community in boreal lakes. In *Ecological Effects of Water-Level Fluctuations in Lakes*; Springer: Heidelberg, Germany, 2008; pp. 13–20.

26. Brauns, M.; Garcia, X.-F.; Pusch, M.T. Potential effects of water-level fluctuations on littoral invertebrates in lowland lakes. In *Ecological Effects of Water-Level Fluctuations in Lakes*; Springer: Heidelberg, Germany, 2008; pp. 5–12.

27. Muneepeerakul, C.P.; Miralles-Wilhelm, F.; Tamea, S.; Rinaldo, A.; Rodriguez-Iturbe, I. Coupled hydrologic and vegetation dynamics in wetland ecosystems. *Water Resour. Res.* **2008**, *44*. [CrossRef]

28. Daly, E.; Porporato, A.; Rodriguez-Iturbe, I. Ecohydrological significance of the coupled dynamics of photosynthesis, transpiration, and soil water balance. *J. Hydrometeorol.* **2004**, *5*, 559–566. [CrossRef]

29. Coops, H.; Hosper, S.H. Water-level management as a tool for the restoration of shallow lakes in the netherlands. *Lake Reserv. Manag.* **2002**, *18*, 293–298. [CrossRef]

30. Ahmadi, R.; Mohebbi, F.; Hagigi, P.; Esmailly, L.; Salmanzadeh, R. Macro-invertebrates in the wetlands of the zarrineh estuary at the south of urmia lake (iran). *Int. J. Environ. Res.* **2011**, *5*, 1047–1052.

31. Stephens, D.W. Changes in lake levels, salinity and the biological community of great salt lake (utah, USA), 1847–1987. In *Saline Lakes*; Springer: Berlin, Germany, 1990; pp. 139–146.

32. Ministry of Agriculture-Jahad. *National Map of Land Use*; Ministry of Agriculture-Jahad: Tehran, Iran, 2001.

33. Petus, C.; Lewis, M.; White, D. Monitoring temporal dynamics of great artesian basin wetland vegetation, australia, using modis ndvi. *Ecol. Indicat.* **2013**, *34*, 41–52. [CrossRef]

34. Mao, D.; Wang, Z.; Luo, L.; Ren, C. Integrating avhrr and modis data to monitor ndvi changes and their relationships with climatic parameters in northeast china. *Int. J. Appl. Earth Obs. Geoinf.* **2012**, *18*, 528–536. [CrossRef]

35. Funderburk, S.L. *Habitat Requirements for Chesapeake Bay Living Resources*; Chesapeake Research Consortium: Annapolis, MD, USA, 1991.

36. Yuan, L.; Zhang, L. Identification of the spectral characteristics of submerged plant *vallisneria spiralis*. *Acta Ecol. Sin.* **2006**, *26*, 1005–1010. [CrossRef]

37. Adam, E.; Mutanga, O.; Rugege, D. Multispectral and hyperspectral remote sensing for identification and mapping of wetland vegetation: A review. *Wetl. Ecol. Manag.* **2010**, *18*, 281–296. [CrossRef]

38. Rouse, J., Jr.; Haas, R.; Schell, J.; Deering, D. Monitoring vegetation systems in the Great Plains with ERTS. In *Goddard Space Flight Center 3d ERTS-1 Symp., Vol. 1, Sect. A*; NASA: College Station, TX, USA, 1974; pp. 309–317.

39. Xu, H. Modification of normalised difference water index (NDWI) to enhance open water features in remotely sensed imagery. *Int. J. Remote Sens.* **2006**, *27*, 3025–3033. [CrossRef]

40. Li, W.; Chen, Q.; Cai, D.; Li, R. Determination of an appropriate ecological hydrograph for a rare fish species using an improved fish habitat suitability model introducing landscape ecology index. *Ecol. Model.* **2015**, *311*, 31–38. [CrossRef]

41. Mozumder, C.; Tripathi, N.; Tipdecho, T. Ecosystem evaluation (1989–2012) of ramsar wetland deepor beel using satellite-derived indices. *Environ. Monit. Assess.* **2014**, *186*, 7909–7927. [CrossRef] [PubMed]

42. Rokni, K.; Ahmad, A.; Selamat, A.; Hazini, S. Water feature extraction and change detection using multitemporal landsat imagery. *Remote Sens.* **2014**, *6*, 4173–4189. [CrossRef]

43. Chen, Y.; Huang, C.; Ticehurst, C.; Merrin, L.; Thew, P. An evaluation of MODIS daily and 8-day composite products for floodplain and wetland inundation mapping. *Wetlands* **2013**, *33*, 823–835. [CrossRef]

44. Ji, L.; Zhang, L.; Wylie, B. Analysis of dynamic thresholds for the normalized difference water index. *Photogramm. Eng. Remote Sens.* **2009**, *75*, 1307–1317. [CrossRef]

45. Zhao, B.; Yan, Y.; Guo, H.; He, M.; Gu, Y.; Li, B. Monitoring rapid vegetation succession in estuarine wetland using time series modis-based indicators: An application in the yangtze river delta area. *Ecol. Indic.* **2009**, *9*, 346–356. [CrossRef]

46. Li, W.; Du, Z.; Ling, F.; Zhou, D.; Wang, H.; Gui, Y.; Sun, B.; Zhang, X. A comparison of land surface water mapping using the normalized difference water index from tm, etm+ and ali. *Remote Sens.* **2013**, *5*, 5530–5549. [CrossRef]

47. Dakos, V.; Carpenter, S.R.; van Nes, E.H.; Scheffer, M. Resilience indicators: Prospects and limitations for early warnings of regime shifts. *Philos. Trans. R. Soc. B Biol. Sci.* **2015**, *370*, 20130263. [CrossRef]

48. Dakos, V.; van Nes, E.H.; Donangelo, R.; Fort, H.; Scheffer, M. Spatial correlation as leading indicator of catastrophic shifts. *Theor. Ecol.* **2010**, *3*, 163–174. [CrossRef]

49. Kuehn, C. A mathematical framework for critical transitions: Bifurcations, fast–slow systems and stochastic dynamics. *Phys. D Nonlinear Phenom.* **2011**, *240*, 1020–1035. [CrossRef]

50. Carpenter, S.R.; Kitchell, J.F.; Hodgson, J.R. Cascading trophic interactions and lake productivity. *BioScience* **1985**, *35*, 634–639. [CrossRef]

51. Dai, L.; Vorselen, D.; Korolev, K.S.; Gore, J. Generic indicators for loss of resilience before a tipping point leading to population collapse. *Science* **2012**, *336*, 1175–1177. [CrossRef] [PubMed]

52. R Development Core Team. *R: A Language and Environment for Statistical Computing*; R Foundation for Statistical Computing: Vienna, Austria, 2013.

53. Naimi, B. RTS: Raster Time Series Analysis. Available online: https://cran.r-project.org/web/packages/rts/index.html (accessed on 4 January 2017).

54. Strogatz, S.H. *Nonlinear Dynamics and Chaos: With Applications to Physics, Biology and Chemistry*; Perseus Publishing: Boulder, CO, USA, 2001.

55. Wissel, C. A universal law of the characteristic return time near thresholds. *Oecologia* **1984**, *65*, 101–107. [CrossRef] [PubMed]

56. Held, H.; Kleinen, T. Detection of climate system bifurcations by degenerate fingerprinting. *Geophys. Res. Lett.* **2004**, *31*, L23207. [CrossRef]

57. Lenton, T.; Livina, V.; Dakos, V.; Van Nes, E.; Scheffer, M. Early warning of climate tipping points from critical slowing down: Comparing methods to improve robustness. *Philos. Trans. R. Soc. A Math. Phys. Eng. Sci.* **2012**, *370*, 1185–1204. [CrossRef] [PubMed]

58. Kendall, M. *Rank Correlation Methods*; Oxford University Press: Oxford, UK, 1962.

59. Bandi, F.M.; Nguyen, T.H. On the functional estimation of jump–diffusion models. *J. Econom.* **2003**, *116*, 293–328. [CrossRef]

60. Carpenter, S.; Brock, W. Early warnings of unknown nonlinear shifts: A nonparametric approach. *Ecology* **2011**, *92*, 2196–2201. [CrossRef] [PubMed]

61. Johannes, M. The statistical and economic role of jumps in continuous-time interest rate models. *J. Financ.* **2004**, *59*, 227–260. [CrossRef]

62. Pace, M.L.; Carpenter, S.R.; Johnson, R.A.; Kurtzweil, J.T. Zooplankton provide early warnings of a regime shift in a whole lake manipulation. *Limnol. Oceanogr.* **2013**, *58*, 525–532. [CrossRef]

63. Seekell, D.A.; Carpenter, S.R.; Cline, T.J.; Pace, M.L. Conditional heteroskedasticity forecasts regime shift in a whole-ecosystem experiment. *Ecosystems* **2012**, *15*, 741–747. [CrossRef]

64. Eslami-Andergoli, L.; Dale, P.; Knight, J.; McCallum, H. Approaching tipping points: A focussed review of indicators and relevance to managing intertidal ecosystems. *Wetl. Ecol. Manag.* **2015**, *23*, 791–802. [CrossRef]

65. Boettiger, C.; Hastings, A. Tipping points: From patterns to predictions. *Nature* **2013**, *493*, 157–158. [PubMed]

66. van Nes, E.H.; Hirota, M.; Holmgren, M.; Scheffer, M. Tipping points in tropical tree cover: Linking theory to data. *Glob. Chang. Biol.* **2014**, *20*, 1016–1021. [CrossRef] [PubMed]

67. Hirota, M.; Holmgren, M.; Van Nes, E.H.; Scheffer, M. Global resilience of tropical forest and savanna to critical transitions. *Science* **2011**, *334*, 232–235. [CrossRef] [PubMed]

68. Filella, I.; Penuelas, J. The red edge position and shape as indicators of plant chlorophyll content, biomass and hydric status. *Int. J. Remote Sens.* **1994**, *15*, 1459–1470. [CrossRef]

69. Dakos, V.; Van Nes, E.H.; D'Odorico, P.; Scheffer, M. Robustness of variance and autocorrelation as indicators of critical slowing down. *Ecology* **2012**, *93*, 264–271. [CrossRef] [PubMed]

70. Smith, A.M.; Kolden, C.A.; Tinkham, W.T.; Talhelm, A.F.; Marshall, J.D.; Hudak, A.T.; Boschetti, L.; Falkowski, M.J.; Greenberg, J.A.; Anderson, J.W. Remote sensing the vulnerability of vegetation in natural terrestrial ecosystems. *Remote Sens. Environ.* **2014**, *154*, 322–337. [CrossRef]